

## Chapter 3

# Dielectric study of homogeneity in some binary liquids in their supercooled state

Interaction among the component molecules of a binary liquid mixture can be studied to some extent by examining the variation of viscosity, refractive index and specific heat with the concentration of the components. However, most of the studies<sup>1-8</sup> are confined to higher temperature range. A better picture of this interaction can be obtained by obtaining additional information about the solid - liquid phase diagrams.<sup>9-12</sup> However, this is not easy with organic liquids, as many of them either cannot be crystallized or in some cases, even if the component liquids are crystallizable, the crystallization is often not complete at the intermediate composition. Thus the determination of the phase diagram<sup>9-12</sup> is severely restricted. Apart from this problem associated with the phase diagram studies, physical properties like viscosity ( $\eta$ ), refractive index ( $n_D$ ), and specific heat  $C_p$  are averaged over the entire binary solution, thus limiting their use. Typical examples are mixtures of an alcohol with alkali halides, which appear to be miscible at room temperature as far as the above mentioned physical properties are concerned; however, the dielectric relaxation measurements reveal micro heterogeneity of a complex nature.<sup>13</sup> Thus, the dielectric study of the binary liquid, especially in the supercooled state,<sup>12-24</sup> has the (additional) advantage of resolving the associated molecular

processes, which, in turn, will help, to a great extent, in determining the phase state of the binary liquid.

When the temperature of the liquid is lowered, the relaxation time (which is of the order of a few picoseconds in the liquid) gets longer until it becomes comparable to that of the experimental time scale. Below this temperature, designated (loosely) as the glass transition temperature  $T_g$ , the liquid no longer responds to the external stresses (as the viscosity is much higher than  $10^{13}$  which is close to that of a solid) and is called "glass". However, the glassy state should not be considered as a completely dead state as relaxation of much smaller magnitude still occur in this state.<sup>25-32</sup> This process is often called the secondary (or  $\beta$ -process) to distinguish it from the primary relaxation process (the  $\alpha$ -process). The origin of  $\beta$ -process in a single component liquid appears to be intramolecular,<sup>28</sup> but in a binary liquid it can even be intermolecular.<sup>25,26,29,30</sup> Because of this in studying the miscibility of the liquids, using dielectric spectroscopy, the  $\beta$ -process has to be taken into consideration.

In a recent paper,<sup>13</sup> we presented our results on a wide variety of H-bonded liquid mixtures. However, with mixtures of non H-bonded liquids, the situation appears to be somewhat different.<sup>16</sup> Here we have critically examined the spectral dependence of relaxation in different types of liquid mixtures in the supercooled state in the context of the miscibility of the liquids and have tried to determine the origin of both  $\alpha$  and  $\beta$ -relaxation processes.

### 3.1. EXPERIMENTAL

The chemicals used in this study are: dl-lactic acid (AR grade, min assay 88%, Std. fine chem., India); dimethylsulfoxide (or DMSO) (Scintillation grade, Spectro Chem., India); acetic acid (glacial, 99-100%, synthesis, Merck, India); cyclohexanol (or CHOH)(LR, Sd. fine chem., India); propylene glycol (or PG)(AR, Sd. fine chem., India); 4-methyl-3-heptanol (or 4M3HOH)(98%, Aldrich Chem. Co., USA); tritolylphosphate

(or TTP)(Sd. fine chem., India); isopropylbenzene (or IPB)( >99%, Merck, Germany); acetone (or ACN) (AR, Spectrochem., India); fluorobenzene (or FB) (99%, synthetic grade, Spectrochem., India); *o*-terphenyl (or OTP) (99%, Aldrich Chem. Co., USA) and diethylphthalate (> 99%, Merck, Germany). All chemicals were used as received. Three kinds of measurements were made on the samples: (1) differential scanning calorimetry (DSC) measurements using a DuPont 2000 Thermal Analyser with a quench-cooling accessory; (ii) dielectric relaxation measurements using a HP4284A Precision LCR Meter in the frequency range of 20 to  $10^6$  Hz; and (iii) dielectric absorption current measurements in the time window of 0.36 to 100 sec using a Keithley Model No. 617 Programmable Electrometer. The glass transition temperatures were determined by using DSC at a heating rate of 10K/min. The details are given in Chapter 2.

## 3.2. RESULTS

### 3.2.1. dl-lactic acid

This acid is widely distributed in nature, which makes it interesting and important. It is usually unstable in its pure form because of self-esterification and hence contains some lactide (cyclic dimer,  $C_6H_8O_4$ ), lactic anhydride [linear polymer or poly (lactic acid)] and water, which is formed in the self-esterification of the acid.<sup>33,34</sup> In order to maintain a high percentage of monomeric lactic acid, it is often made available as 85-88% in aqueous solution.<sup>33(b)</sup> The sample used in the present study, according to the manufacturer's specification, has a minimum assay of 88%. To obtain some idea of the amount of water added by the manufacturer, we have measured the refractive index( $n_D$ ) of the sample with an Abbe Refractometer. The value is 1.4255 at 293.15K. The density ( $\rho$ ) of the sample, as specified by the manufacturer is, 1.200 to 1.206 g-cm<sup>-3</sup> at the same temperature. We have used the values of  $n_D$  and  $\rho$  of the aqueous solution (given in Refs. 1 and 33), to estimate the amount of water, which turns out to be *ca.* 12%, which tallies with the specifications of the manufacturer. We used the sample as received without

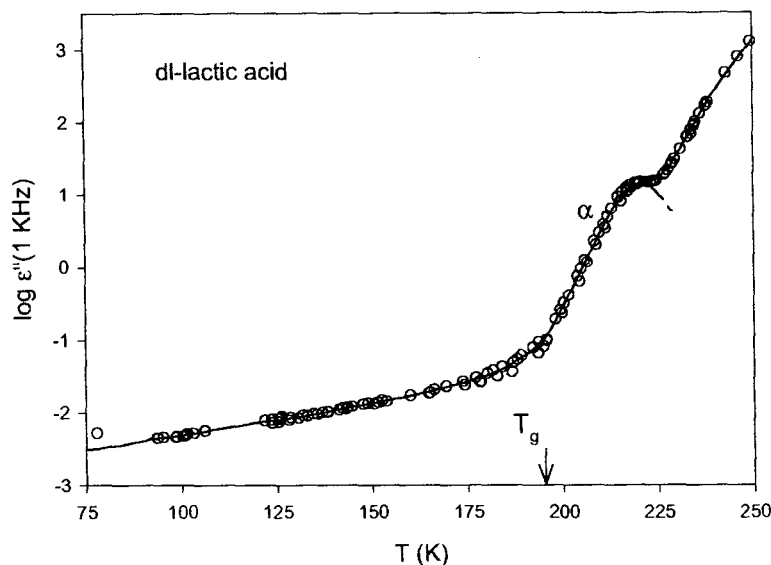
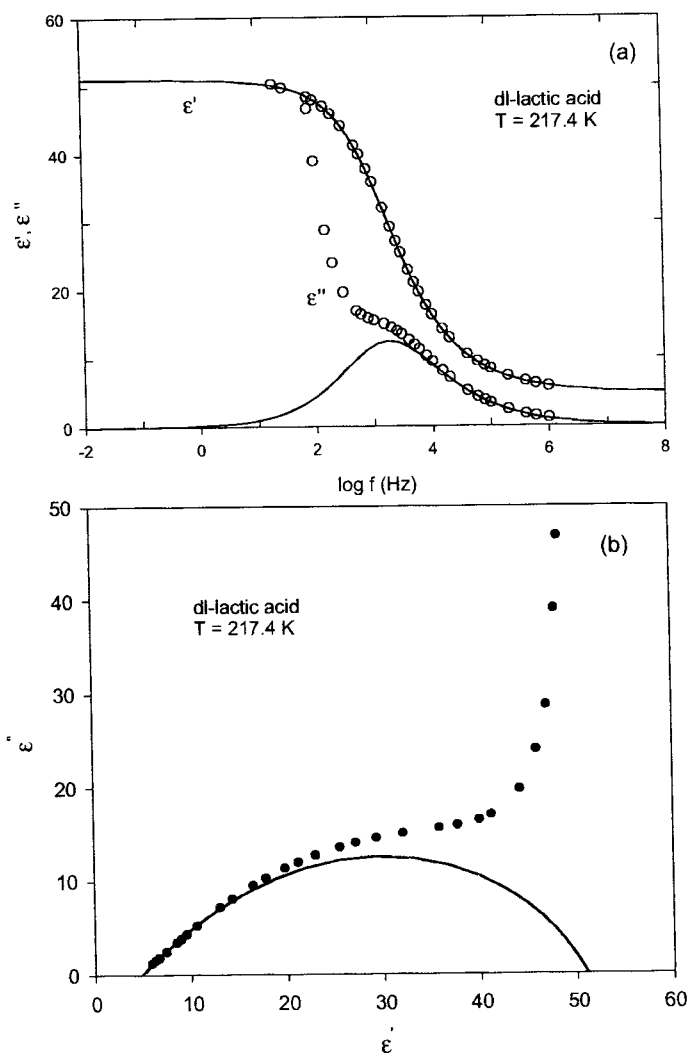


Figure 3.1: Variation of  $\log \epsilon''$  at 1 KHz test frequency with temperature in supercooled dl-lactic acid.

further purification, as our effort to study a purified sample did not give us very reliable values probably because of the self-estrification during the measurements. The dielectric properties also could not be studied because of crystallization and high ionic conductivity with more purified sample. Hence, we again used the material as- received, which is stable against crystallization during the experiments. This sample was earlier studied in its 'near pure' form (where the purity was found to be dependent on the sample history) and with different sample histories by Parks *et al.*<sup>34</sup> both in the liquid and crystalline states. The same data were used later by Privalko<sup>35</sup> to determine the entropies of both of the states. The glass transition (defined as the onset of the glass-forming process) for this sample is about  $195\text{-}200\text{K}$ <sup>34</sup> and the corresponding zero excess entropy temperature (or the Kauzmann temperature,  $T_K$ ) has been found to be  $182\text{K}$ <sup>35</sup>. The difference of 18 degrees between these two temperatures has evoked some interest in this liquid, in view of the imminent Kauzmann entropy paradox in very fragile liquids (for details see Refs. 36-40). The interest in this material is because of the fact that it can be classified<sup>38</sup> as a very fragile liquid on the basis of the change of specific heat at  $T_g$ . The  $T_g$  measured for our sample using DSC for a heating rate of 10 K/min is 194.2 K (about 6 degrees lower than that of Parks *et al.*). The dielectric measurements were performed in the



**Figure 3.2:** Dielectric relaxation in supercooled dl-lactic acid at  $T = 217.4 \text{ K}$ . (a) Variation of  $\epsilon'$  and  $\epsilon''$  with  $\log f$ . The open symbol corresponds to the experimental points. The solid lines correspond to Eq. (1.41) with  $\alpha_{HN} = 0.297$ ,  $\beta_{HN} = 0.722$ ,  $f_0 = 1.22 \times 10^3 \text{ Hz}$ ,  $\epsilon_0 = 51.06$  and  $\epsilon_\infty = 4.90$ . (b) Cole - Cole diagram. The solid line corresponds to Eq. (1.41) given in (a).

supercooled liquid and glassy states down to a temperature of 77 K. The variation of dielectric loss  $\epsilon''$  at 1 KHz test frequency with temperature shown in Figure 3.1 reveals only one dielectric process, which can be identified with the  $\alpha$ -relaxation. There is no evidence of secondary relaxation. The spectral shape dependence of  $\epsilon'$  (real part of the complex dielectric constant  $\epsilon^*$ ) and  $\epsilon''$  (imaginary part of  $\epsilon^*$ ) of the  $\alpha$ -process at a 217.4 K are shown in Figure 3.2(a) and the corresponding Cole-Cole diagram is shown in Figure 3.2(b). We are able to describe the real part of the permittivity by extracting the real part from the Havriliak-Negami equation<sup>41</sup>. [Eq. (1.41)] The dielectric loss data contained some contribution from direct conduction (dc) losses.

**Table I. Details of  $\alpha$  processes in dl-lactic acid**

$T^a$	$\alpha_{HN}$	$\beta_{HN}$	$\log f_0$	$\epsilon_0$	$\epsilon_\infty$	$\log f_m$
245.5	0.209	0.698	6.02	43.28	3.40 <sup>b</sup>	6.29
238.4	0.267	0.731	5.55	45.16	3.40 <sup>b</sup>	5.79
227.5	0.255	0.691	4.40	47.80	4.90 <sup>b</sup>	4.68
217.4	0.294	0.717	3.09	50.93	4.89	3.34
215.0	0.220	0.600	2.30	53.00	4.60	2.65
211.7	0.200	0.600	1.95	50.00	4.60	2.29
200.3	—	—	—	—	—	-1.84 <sup>c</sup>
196.0	—	—	—	—	—	-2.60 <sup>c</sup>

a Absolute temperatures K.

b Extrapolated values for the best fits; Hence, all values are very approximate.

c From time domain measurements.

In order to eliminate the dc loss from the total dielectric loss, we made use of the Kramers - Kronig relation as described in Ref. 42 (and also in Ref. 43) to obtain the dipolar contribution. One can also eliminate the dc loss by using the complex conductivity plot described by Grant.<sup>44</sup> We used both the methods and obtained the same result, within experimental uncertainty. The resolved dipolar loss is shown in Figure 3.2(a); the result Cole-Cole diagram is shown in Figure 3.2(b).

**Table II. Fitting Eqs. (1.53, 1.54) to Dielectric data on dl-lactic acid**

$T_g$ (K)	$T_K^*$ (K)	Fitting parameters			
194.1	182.0	Eq. 1.54	$\log A = 12.53$	$r = 11.85$	$T_g' = 187.3K$
		Eq. 1.53	$\log f_{0,\alpha} = 11.91$	$B = 1007.3$	$T_0 = 167.2K$

The  $\epsilon''$  thus resolved at different temperatures fits, as expected, the same parameters of Eq. (1.41) that describe  $\epsilon'$ . The details of the  $\alpha$ -process for this sample are given in Table I. We have obtained the peak loss frequency  $f_m$  from the parameters shown in Table I, using the relation given in our earlier publication.<sup>15</sup> These values of  $f_m$  together with  $f_m$  values obtained using the time-domain technique on the lower-frequency side, are found to follow the Power - Law (PL) equation<sup>38,39</sup> (1.54).

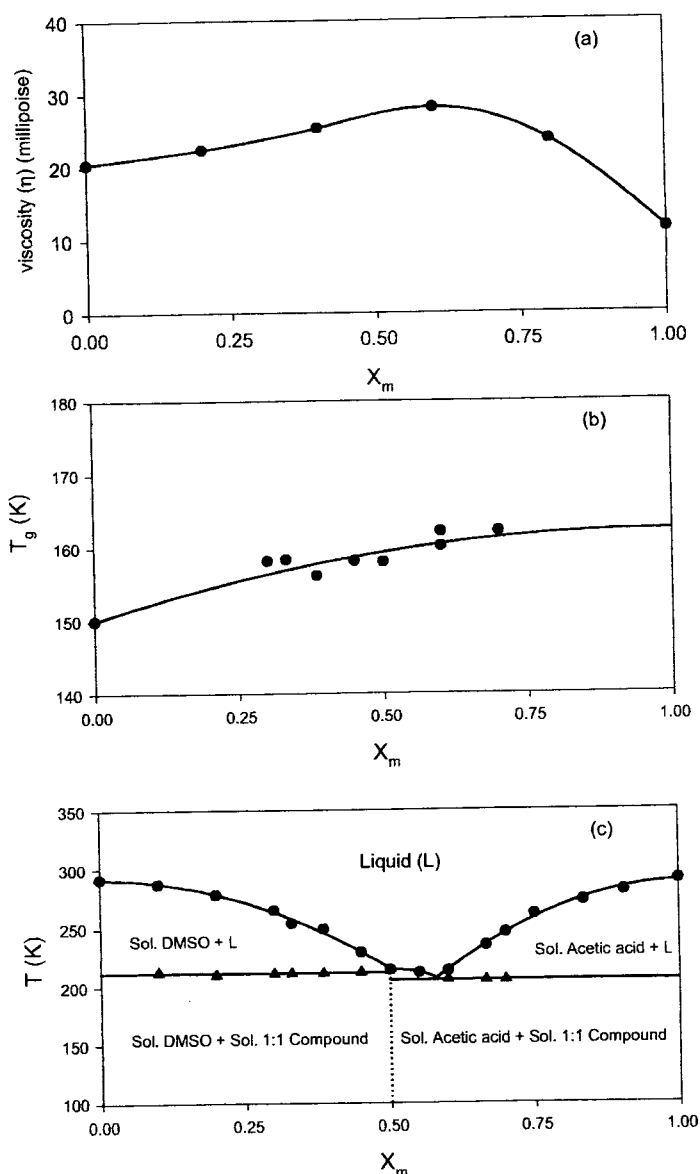


Figure 3.3: Variation of (a) viscosity and (b) glass transition temperature  $T_g$  with mole fraction  $x_m$  of acetic acid in DMSO - acetic acid mixtures. The solid line in (b) is given by Eq. (1.2) with  $T_{g1} = 150.0$ ,  $T_{g2} = 162.3$  and  $k = 12.65$ . The value of  $T_g$  for pure DMSO in Eq. (1.2) is taken from our earlier study<sup>10,15</sup> determined using the method of extrapolation of the binary liquid data. Also shown in (c) is the solid - liquid phase diagram. Note that there is evidence for a compound formation at  $x_m = 0.50$ . The solid lines along the liquidus points are given Eqs. (1.41, 1.54) for the parameters given in the text.

The Vogel - Fulcher - Tammans (VFT) equation<sup>10,36,39</sup> (1.53) is also found to adequately describe the same data within the experimental uncertainties of  $f_m$  values. Here  $T_0$  is the limiting glass transition temperature. The pre-exponential factor  $f_{0,\alpha}$  may be identified with the lattice vibrational frequency. The parameters corresponding to Eqs. (1.53, 1.54) are given in Table II.

### 3.2.2. DMSO-Acetic Acid Mixtures

DMSO is known to interact strongly with water<sup>2,4,10,15,45,46</sup> [more than with alcohols<sup>45</sup>], but the nature of its interaction with acetic acid is not clearly known. The dielectric relaxation data of Wessels *et al.*<sup>47</sup> of DMSO-acetic acid mixtures at 293.15 K reveals a low frequency feature which they ascribe to a 1:1 heteroassociates. The viscosity data of Fort and Moore<sup>2</sup> in these mixtures show a strong interaction in intermediate concentration regions. This situation is shown in Figure 3.3(a) where the viscosity data of Fort and Moore is plotted against concentration. Interestingly, the liquid mixtures at these concentrations supercool to form glasses, although both DMSO and acetic acid are poor glass formers on their own. This situation is shown in Figure 3.3(b) where we have shown the  $T_g$  values measured at a heating rate of 10 K/min, for these concentrations. The details of the  $T_g$  measured are given in Table III for all of the materials studied here. The  $T_g$  of the liquid mixtures follows the equation<sup>10</sup> (1.2).

**Table III.  $T_g$  Data for the Liquids Studied**

	Sample	$T_g^b$
1	dl-lactic acid (88 % in aqueous solution)	194.1
2	DMSO-acetic acid $x_m = 0.500$	158.0
	$x_m = 0.588$	159.7
3	PG-CHOL $x_m = 0.333$	168.2
	$x_m = 0.688$	163.4
4	4M3H0H-TTP $x = 0.106$	165.3
5	IPB $x = 0.000$	130.8
6	IPB-FB $x = 0.100$	131.2
7	IPB-ACN $x = 0.101$	129.3
8	OTP-DEP $x = 0.100$	229.3

b Absolute temperatures K.



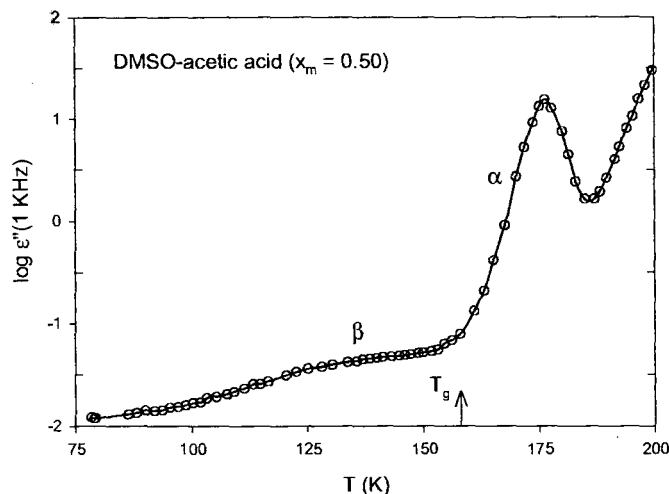


Figure 3.4: Variation of  $\log \epsilon''$  at 1 KHz test frequency with temperature in supercooled DMSO - acetic acid for  $x_m=0.50$ . The solid line is guide to the eye.

We have partly succeeded in crystallizing the DMSO-acetic acid binary liquids to determine the solid - liquid phase diagram using DSC, as mentioned in our earlier references.<sup>10,11,15</sup> The resulting phase diagram is shown in Figure 3.3(c) shows 1:1 compound formation, which strongly supports the earlier view of Wessels *et al.*<sup>47</sup> We were able to study the supercooled mixtures in the mole fraction ( $x_m$ ) region of  $0.5 \leq x_m \leq 0.6$  using dielectric spectroscopy. We have studied the mixtures with  $X_m$  values of 0.500 and 0.588. The temperature variation of  $\epsilon''$  at test frequency of 1 KHz with temperature is shown in Figure 3.4 for  $x_m=0.500$ , which clearly reveals two relaxations identified as  $\alpha$ - and  $\beta$ -processes. Typical spectral dependence of the  $\alpha$ - and  $\beta$ -processes in these mixtures are shown in Figure 3.5 in the form of Cole-Cole diagrams. The corresponding Arrhenius diagram is plotted in Figure 3.6, where we have also shown the room temperature data of pure liquids,<sup>48,49</sup> for the purpose of comparison.

### 3.2.3. PG-CHOH Mixtures

These mixtures form glass easily, up to about 0.80 weight fraction of CHOH.<sup>51</sup> The  $T_g$  of the liquid mixture has been found to follow Eq. (1.2) with  $T_{g1} = T_g(PG) = 172.9$  K

$T_{g2} = T_g(\text{CHOH}) = 158.6$  K and  $k = 0$ . Eq. (1.2) is often used by researchers to estimate the liquid  $T_g$  for a non-glass forming liquid, such as CHOH (for details on this

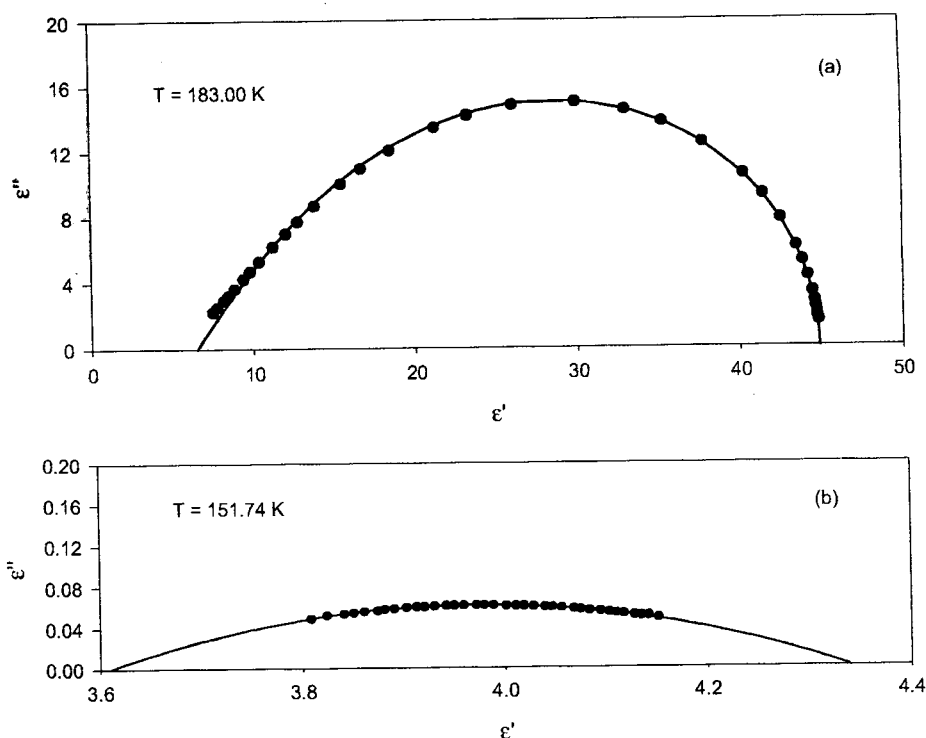


**Figure 3.5:** Cole-Cole diagrams corresponding to the temperatures above and below  $T_g$  in DMSO - acetic acid mixtures with  $x_m=0.50$ . (a) Relaxation at  $T= 183.00$  K showing the prominent  $\alpha$ -process. The solid line corresponds to Eq. (1.41) with  $\alpha_{HN}= 0.01$ ,  $\beta_{HN}= 0.624$ ,  $f_0= 1.133 \times 10^4$  Hz,  $\epsilon_0= 44.85$  and  $\epsilon_\infty= 6.59$ . (b) Relaxation at  $T=151.74$  K, showing the  $\beta$ -process. The solid line corresponds to Eq. (1.41) with  $\alpha_{HN}= 0.788$ ,  $\beta_{HN}= 1$ ,  $f_0 = 1.755 \times 10^4$  Hz,  $\epsilon_0= 4.34$  and  $\epsilon_\infty= 3.61$ .

the reader may consult Refs. 50 and 51). However, what is not clear is the reliability of this method for estimating  $T_g$ , as we have no idea about the homogeneity of these mixtures. With this in mind, we have critically examined the various relaxation processes in these mixtures at three concentrations of CHOH down to 77 K. The temperature variation of  $\epsilon''$  at test frequency of 1 KHz (Figure 3.7) shows only one relaxation process above  $T_g$ , which can be identified with the  $\alpha$ -process. No sub- $T_g$  process is found in these mixtures. The spectral shape dependence of the  $\alpha$ -relaxation is shown in Figure 3.8; the corresponding Arrhenius diagram is shown in Figure 3.9.

### 3.2.4. 4M3HOH - TTP mixtures

In a recent article from our laboratory<sup>13</sup> that, even in mixtures of an alcohol and a non-H-bonded liquid, which are miscible at room temperature, a microheterogeneity at low temperatures may be revealed by dielectric relaxation. It is with this in mind that we have studied the 4M3HOH - TTP mixture. These were particularly chosen because

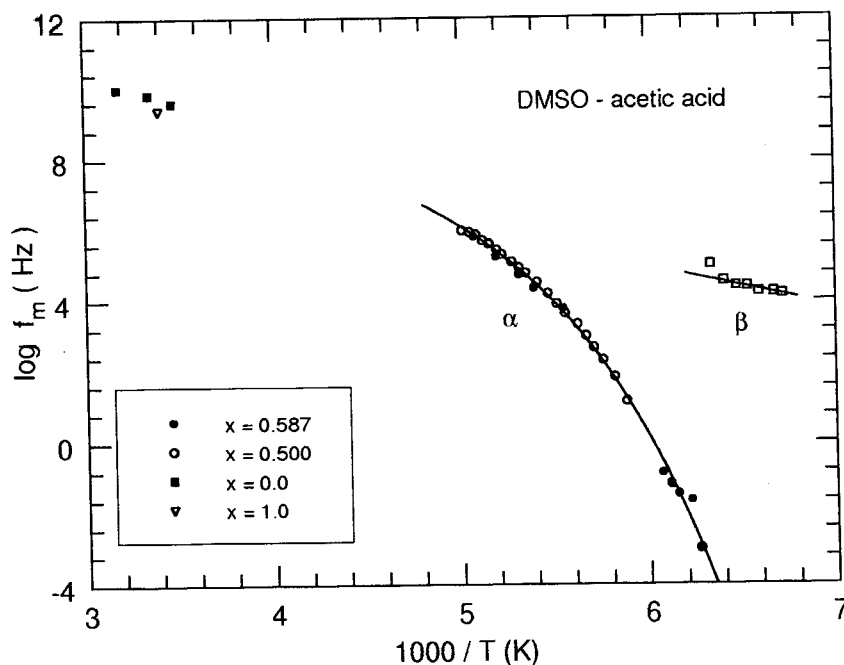


Figure 3.6: Arrhenius diagram for DMSO - acetic acid mixtures. Also shown in the diagram are the room temperature data taken from Refs.48 and 49 for the pure components. Also shown are the corresponding  $T_g$  values given by ( $\oplus$ ), which correspond to an approximate enthalpy relaxation frequency of  $10^{-3}$  Hz.

both are known to be non - crystallizable and 4M3HOH unlike the other octanols viz. 2-ethylhexanol, prefers a ring conformation as opposed to the chain conformation in 2-ethylhexanol. For this reason the dielectric spectrum shows<sup>51</sup> very little dispersion, thus, facilitating analysis. The temperature variation of  $\epsilon''$  at 1 KHz for 4M3HOH with 10.0% of TTP by weight, is shown in Figure 3.10, along with the data for pure 4M3HOH. No clearly resolvable sub- $T_g$  process has been noted and there is only one process for temperatures above  $T_g$ . On a close examination of the data, we find that the peak in Figure 3.10 is due to a superposition of two processes. This can be seen very clearly in Figure 3.11, where we give the corresponding data at various temperatures above  $T_g$  in the form of Cole-Cole diagrams. One can see the presence of a smaller high frequency process on the lower- $T$  side, which is resolved from the dominant process using superposition. Resolved  $f_m$  values of these processes are shown in Figure 3.12 in the form of an Arrhenius diagram, along with the  $f_m$  values of the pure components.

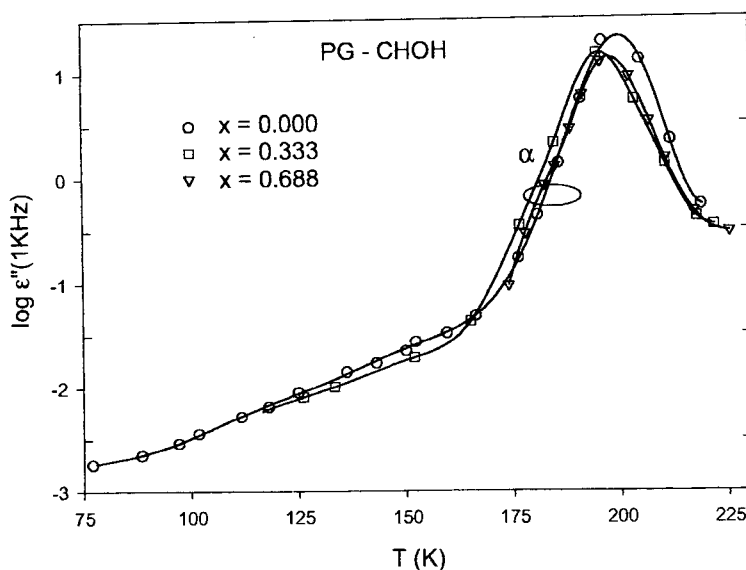


Figure 3.7: Temperature variation of dielectric loss  $\epsilon''$  at 1KHz test frequency for various weight fractions ( $x$ ) of CHOH in supercooled PG - CHOH mixtures.

### 3.2.5. Mixtures of non- $H$ -bonded liquids:

#### 3.2.5.1. Mixtures of IPB with ACN and FB

It is the practice in the field of dielectrics to study non-polar liquids by using small quantities of dipolar solutes<sup>16,25-27,30,48</sup> as probes. By supercooling the mixtures, the relaxation of the dipolar molecule has been found to occur at lower frequencies and to split into two processes one is the primary (or  $\alpha$ -)relaxation, which freezes at  $T_g$  and the other of much smaller magnitude, is the  $\beta$ -process, which continues to the sub- $T_g$  region. The origin of  $\alpha$ -process lies in the cooperative relaxation of the dipolar solute along with the non-polar solvent molecules. However, what is not clear is why the  $\alpha$ -process in binary mixtures is generally broader than that usually found in monomeric liquids.<sup>25-27,30</sup> In order to answer this question, we have critically examined the mixtures of slightly polar IPB with strongly polar liquids in small quantities. The results are presented in Figures 3.13-3.16.

Shown in Figure 3.13 is the temperature variation of the corresponding dielectric loss  $\epsilon''$  at a test frequency of 1 KHz which reveals both  $\alpha$ - and  $\beta$ -processes. Figure 3.14 and 3.15 are the Cole-Cole diagrams corresponding to the  $\alpha$ - and  $\beta$ -processes in these liquids. The complete Arrhenius diagram of these samples is shown in Figure 3.16.

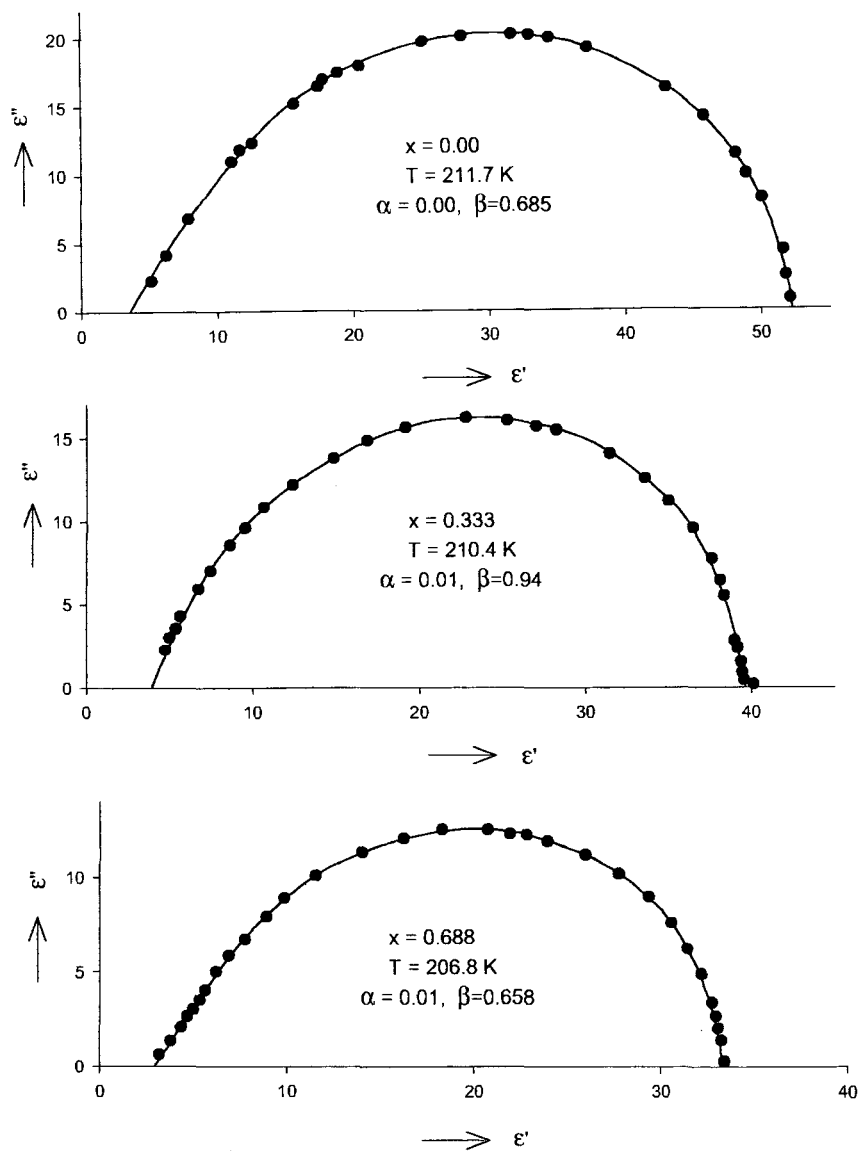


Figure 3.8: Cole-Cole diagrams at temperatures above  $T_g$  in various PG - CHOH mixtures. Also shown along the curves are the corresponding parameters of Eq. (1.41).

### 3.3. DISCUSSION

For convenience, we discuss each set of mixtures separately.

**3.3.1** In the case of dl-lactic acid, the spectral dependence of the complex dielectric constant, as shown in Figure 3.2 and Table I, shows that the symmetric distribution parameter  $\alpha_{HN}$  of Eq. (1.41) is large. Most of the monomeric liquids studied<sup>28,52,53</sup> by us did not show such large  $\alpha_{HN}$  values. It is very difficult for us to say, at this stage, whether the very large  $\alpha_{HN}$  is due to the presence of water (as discussed in the results section) or is due to polymeric entities present in the liquid. The other interesting

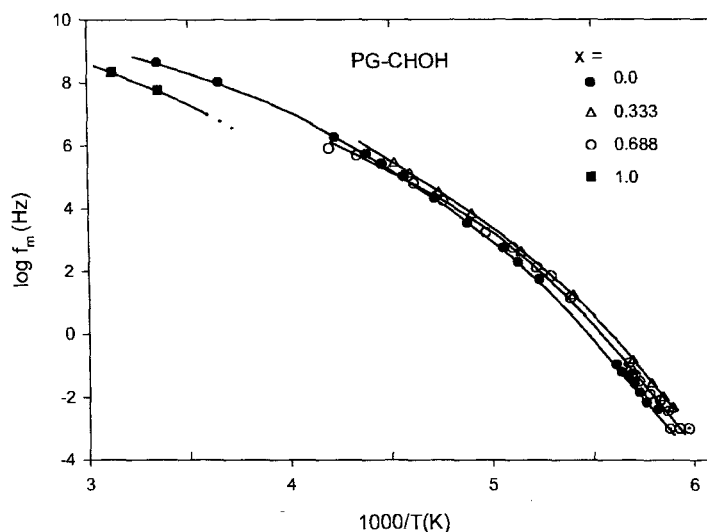


Figure 3.9: Arrhenius diagram for PG - CHOH mixtures. In addition are data at higher temperatures taken from the Ref.48. Also shown ( $\odot$ ) are the corresponding  $T_g$ 's [Table III] which correspond to the approximate enthalpy relaxation frequency of  $10^{-3}$  Hz.

aspect of this liquid relaxation is that if the primary relaxation is fitted to Eq. (1.54), the relaxation frequency approaches zero at a temperature ( $T_g$ ) of 187.3 K which is nearly the same as the Kauzmann temperature ( $T_K$ ) of 182K (Table II), whereas the limiting temperature  $T_0$  of the VFT equation, Eq. (1.53), falls much below  $T_K$ , indicating that the former is perhaps a better representation of the T- dependence of  $f_m$ .

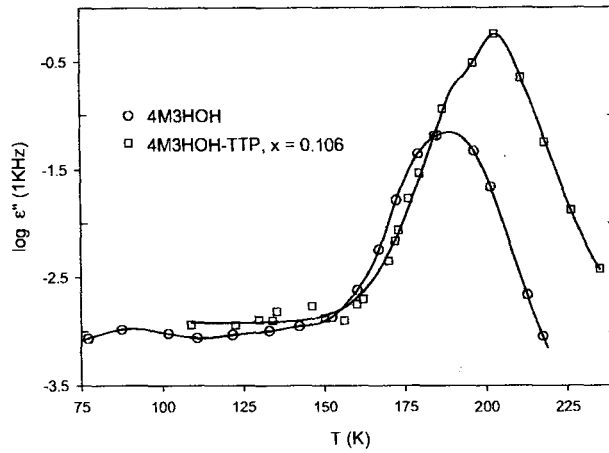


Figure 3.10: Temperature variation of dielectric loss  $\epsilon''$  at 1KHz test frequency in supercooled 4M3HOH - TTP mixture with weight fraction ( $x$ ) of TTP of 0.106. Also shown are the corresponding data<sup>52</sup> of pure 4M3HOH for comparison.

Interestingly, there is no evidence of  $\beta$ -process in this liquid and the sub- $T_g$  region reveals a relaxation behaviour typical of lattice relaxation.<sup>43</sup> In essence, our results reveal that the dl-lactic acid with the intentionally added water, is a homogeneous mixture.

**3.3.2.** In the case of DMSO - acetic acid, our phase diagram study, although not complete, indicates a stable 1:1 complex formation at low temperature. The liquidus lines shown in the phase diagram can be described by assuming 1:1 complex formation and by using the approximate expression for the depression of the freezing point given by the equation,<sup>8</sup>

$$-\ln x_m = \frac{\Delta H_{m2}}{R} \left( \frac{1}{T_2} - \frac{1}{T_{m2}} \right) \quad (3.1)$$

for the acetic acid rich side, and

$$-\ln(1 - x_m) = \frac{\Delta H_{m1}}{R} \left( \frac{1}{T_1} - \frac{1}{T_{m1}} \right) \quad (3.2)$$

for the DMSO-rich side. In the above equation,  $T_1$ ,  $T_2$  are the corresponding liquidus temperatures;  $T_{m1}$ ,  $T_{m2}$  are the corresponding melting temperatures of the pure components and  $\Delta H_m$ 's are the corresponding enthalpies of fusion. We have taken the values of  $\Delta H_m$ 's for these liquids from Ref. 33(a). The values of  $\Delta H_m$ 's are: 12500 J/mol for DMSO and 8000 J/mol for acetic acid. These values are used to describe the liquidus lines using Eqs. (3.1,3.2) by assuming a 1:1 complex formation [see Figure 3.3(c)].

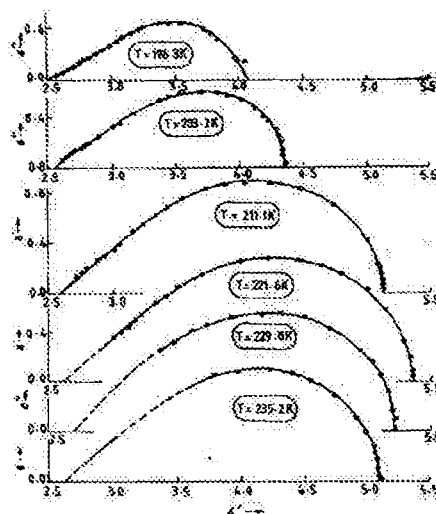


Figure 3.11: Cole-Cole diagrams at various temperatures above  $T_g$  in 4M3HOH - TTP mixture ( $x=0.106$ ). Note the presence of two processes at lower temperatures.

This confirms the existence of stable complexes, even in the liquid state; this view is also supported by the dielectric studies of Wessels *et al.*<sup>47</sup> The corresponding dielectric relaxation shown in Figure 3.5(a) shows a simple Cole-Davidson form [ $\alpha_{HN}=0$  in Eq. (1.41)] of relaxation indicating a homogeneity of the liquid. There is also a  $\beta$ -process, as shown in Figure 3.5(b), with a considerable amount of polarization. However, the loss peaks could be well resolved only in a very narrow temperature range (Figure 3.6) and the corresponding activation energies could not be estimated. Hence, the origin of this  $\beta$ -process could not be ascertained. In this context, is the of Fort and Moore.<sup>2</sup> The viscosity vs. concentration curves of DMSO with acetonitrile and with methanol do not reveal peak. However, the curves for DMSO mixtures with acetic acid and with water clearly reveal them. We have carried out a study of solid - liquid phase diagram for all four systems. The data of DMSO - acetonitrile and DMSO - methanol reveal simple eutectic phase diagrams (unpublished result from this laboratory).<sup>2</sup> Recent study from our laboratory<sup>10,15</sup> on DMSO - water and the present study of DMSO - acetic acid clearly indicates complex formation in the solutions; this observation is in line with the studies of Drinkard and Kivelson<sup>45</sup> and Fort and Moore<sup>2</sup>.



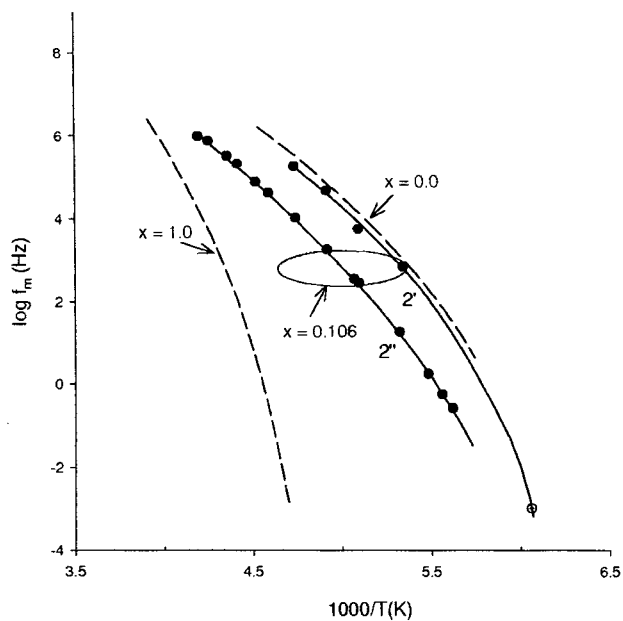


Figure 3.12: Complete Arrhenius diagram for 4M3HOH - TTP mixture with  $x=0.106$ . The  $f_m$  values corresponding to the pure components are taken from our earlier studies.<sup>52,53</sup>

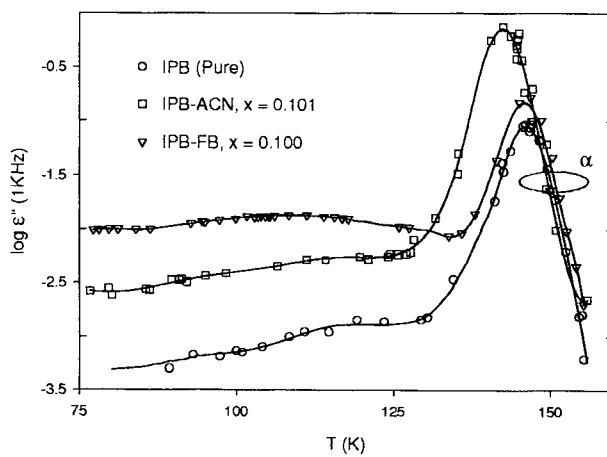


Figure 3.13: Temperature variation of dielectric loss  $\epsilon''$  at 1 KHz test frequency in binary mixtures of FB and ACN in IPB. Also shown are the pure IPB data for comparison.

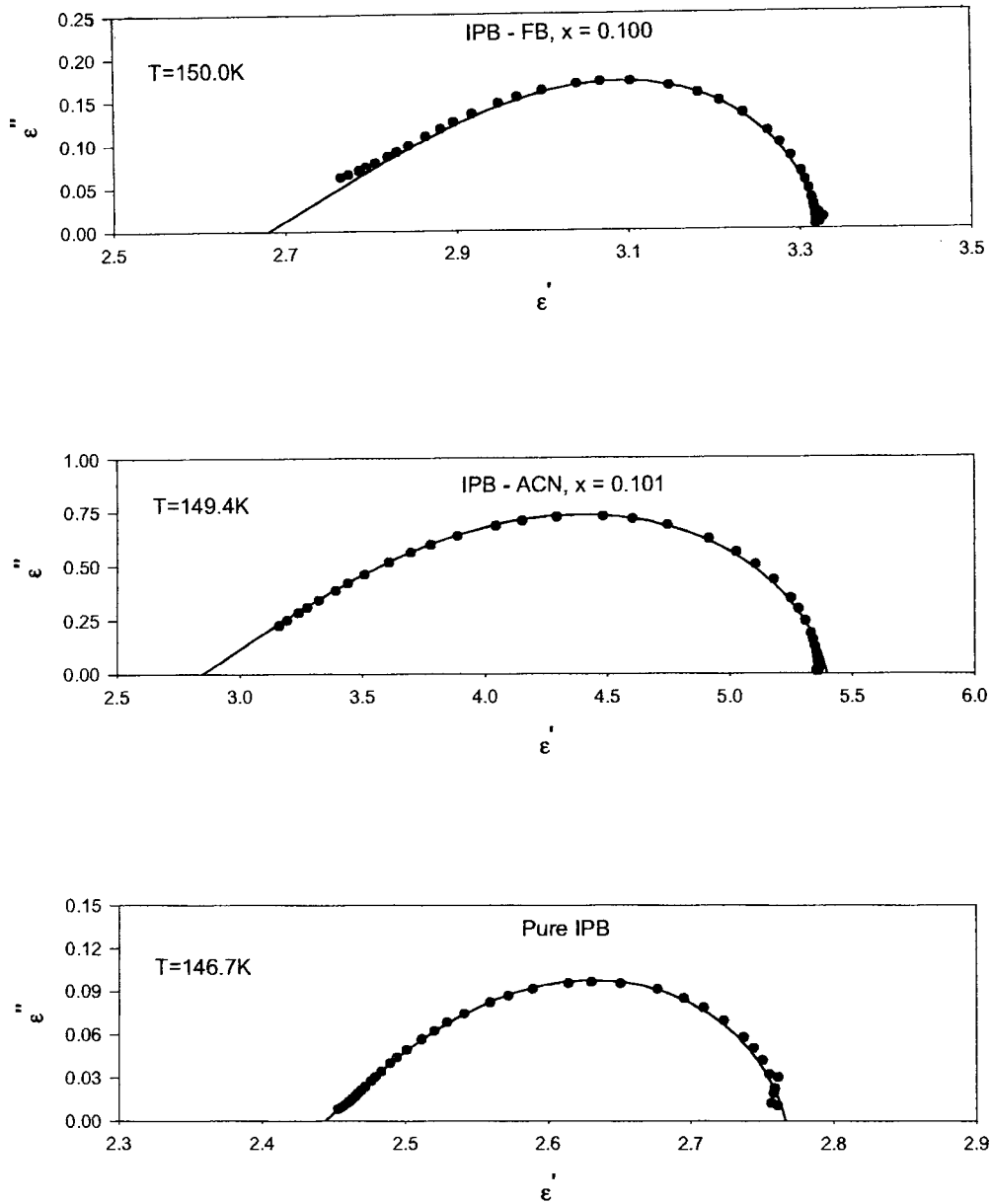
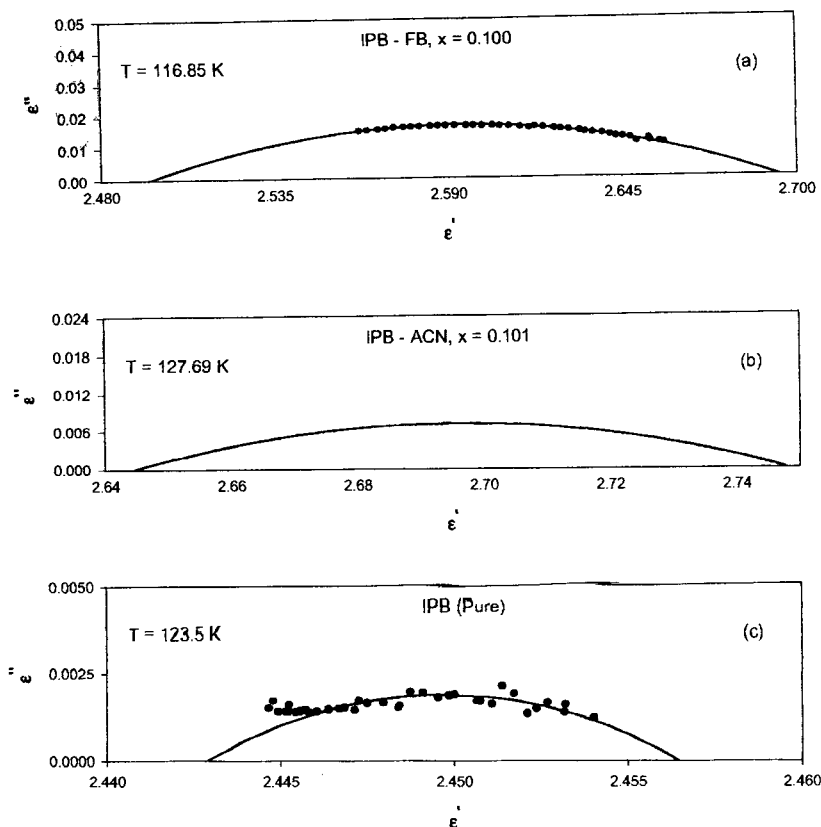


Figure 3.14: Cole-Cole plots at the specified temperatures above  $T_g$  in mixtures of IPB with FB and ACN. Also shown are the pure IPB data for comparison. The solid lines correspond to Eq. (1.41) for the following parameters: (1) IPB - FB,  $x = 0.100$ :  $\alpha_{HN} = 0.115$ ,  $\beta_{HN} = 0.470$ ,  $f_0 = 1.132 \times 10^4$  Hz,  $\epsilon_0 = 3.320$  and  $\epsilon_\infty = 2.730$ ; (ii) IPB - ACN,  $x = 0.101$ :  $\alpha_{HN} = 0.127$ ,  $\beta_{HN} = 0.480$ ,  $f_0 = 1.585 \times 10^3$  Hz,  $\epsilon_0 = 5.400$  and  $\epsilon_\infty = 2.850$ ; (iii) IPB (pure):  $\alpha_{HN} = 0.152$ ,  $\beta_{HN} = 0.562$ ,  $f_0 = 1.057 \times 10^3$  Hz,  $\epsilon_0 = 2.768$  and  $\epsilon_\infty = 2.448$ .



**Figure 3.15:** Cole-Cole plot corresponding to the sub- $T_g$  temperatures in the mixture of IPB with FB and with ACN. The solid lines correspond to Eq. (1.41) for the parameters: (a) IPB - FB,  $x = 0.100$ :  $\alpha_{HN} = 0.788$ ,  $\beta_{HN} = 1.000$ ,  $f_0 = 6.070 \times 10^4$  Hz,  $\epsilon_0 = 2.694$  and  $\epsilon_\infty = 2.495$ ; (b) IPB - ACN,  $x = 0.101$ :  $\alpha_{HN} = 0.826$ ,  $\beta_{HN} = 1.000$ ,  $f_0 = 1.950 \times 10^4$  Hz,  $\epsilon_0 = 2.748$  and  $\epsilon_\infty = 2.645$ ; (c) IPB (pure):  $\alpha_{HN} = 0.657$ ,  $\beta_{HN} = 1.000$ ,  $f_0 = 4.663 \times 10^3$  Hz,  $\epsilon_0 = 2.456$  and  $\epsilon_\infty = 2.443$ .

**3.3.3.** The PG - CHOH mixtures show a much broader loss peaks for  $x_m = 0.33$  resulting in non-zero values of  $\alpha_{HN}$ , whereas for the other concentrations, the spectra are of simple Cole-Davidson type ( $\alpha_{HN} = 0$ ). These broad loss peaks for  $x_m = 0.33$  are, perhaps due to a microscopic heterogeneity, whereas on the CHOH rich side the spectrum is homogeneous. Interestingly, these mixtures do not reveal a  $\beta$ -process (Figure 3.7).

**3.3.4.** In 4M3HOH - TTP mixtures, the components of the liquids are miscible at room temperature and the DSC results show a single  $T_g$  for the liquid mixtures [Table III]. However, the dielectric relaxation of this mixture presented in Figure 3.11 as Cole-Cole diagram shows a relaxation of Cole-Davidson type. A critical examination of the variation of  $\epsilon_0$  with temperature in Figure 3.11, reveals that some component of the liquid containing the polar TTP molecules is freezing (kinetically) on lowering the

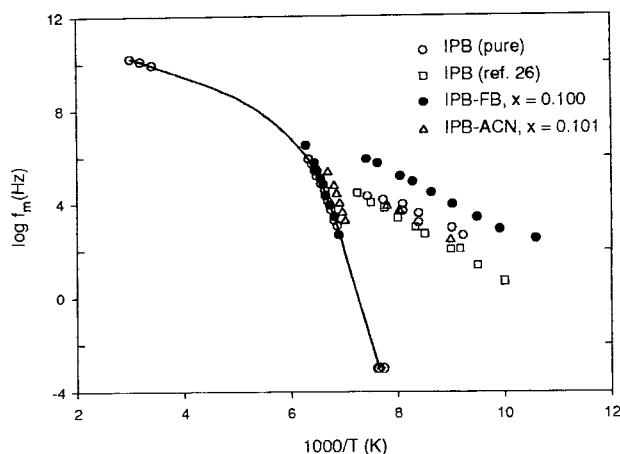


Figure 3.16: Complete Arrhenius diagram for mixtures of IPB with FB and with ACN. Also shown (o) in the diagram are the room temperature data<sup>Ref.18</sup> for IPB. Also included is the data of Johari and Goldstein<sup>Ref.26</sup> on IPB for comparison purpose. The points shown by (⊕) correspond to the  $T_g$  values measured by the DSC.

temperature and a second process is clearly seen on the lower temperature side, whose  $f_m$  values (resolved approximately) are much closer to pure 4M3HOH, as shown in Figure 3.12. In this figure the two  $\alpha$ -processes under discussion are labeled as  $2''$  as  $2'$ . Thus, it appears that there is a micro-heterogeneity in the sample where in the above two processes correspond to different liquid regions. The composition of the liquid mixtures appears to be varying continuously as the temperature is lowered. This behaviour is similar to that of 1-bromobutane in 2-ethylhexan-1-ol, discussed in our recent article.<sup>13</sup>

**3.3.5.** In mixtures of non  $H$ -bonded binary liquids, the dielectric spectrum is generally found to be broader than that of the main component in its pure form. This can be seen in Figure 3.14. This, in our view, is due to the distribution of environments around the dipolar solute molecule arising because of a non uniform distribution of the solute molecules in the solvent. The solution may, however, be regarded more or less as a homogeneous liquid on a macroscopic scale.

**3.3.6.** Although, the main aim of this study is not the  $\beta$ -relaxation process, we wish to make a few observations regarding this process. The  $\beta$ -relaxation in IPB - FB mixtures is clearly due to the rotation of FB in an otherwise rigid (glassy) matrix. The freedom of rotation of FB in the glassy state is greater than that of ACN.

Thus, one can treat the  $\alpha$ -process as due to the cooperative large-angle rotation of the solute molecules along with that of the solvent molecules and the  $\beta$ -process may be treated as due to a small-angle rotation of the FB molecule within the frozen matrix.<sup>31</sup> The magnitude of  $\beta$ -relaxation in binary liquids, thus, depends on the size and shape of the solute molecule with reference to the solvent molecule.<sup>29,30</sup> The origin of  $\beta$ -relaxation in DMSO - acetic acid is difficult to determine at this stage; however, in this context, it is interesting to see that, the H-bonded liquid mixtures, in general, do not reveal a clearly resolvable  $\beta$ -process (Figures 3.1,3.7 and 3.10) and also have a very high  $\epsilon_\infty$  value in the glassy state, that is much in excess of  $1.05 n_D^2$  (see Figures 3.5(b) and 3.8). This aspect needs to be probed further.

### 3.4. CONCLUSIONS

Our study indicates homogeneity in the mixtures of similar types of liquids, viz., two H-bonded or two non H-bonded liquids down to their respective glass transition temperatures (which is not found to be true in the case of two dissimilar liquids like 4M3HOH + TTP). The dielectric relaxation spectra above  $T_g$  (i.e.,  $\alpha$ -process) is slightly broader in the case of non H-bonded liquid mixtures like FB+IPB, etc., as compared to two H-bonded liquids. Our study on DMSO-acetic acid mixtures clearly indicates 1:1 complex formation in the supercooled region.

The other interesting aspect that has emerged out of our study is the near absence (or weak)  $\beta$ - or secondary relaxation process in liquid mixtures of two H-bonded liquids.

### 3.5. References

1. J. Timmermans, *The Physico - Chemical Constants of Binary Systems in Concentrated Solutions* [Wiley(Inter Science), New York, 1960].
2. R. J. Fort and W. R. Moore, *Trans. Faraday Soc.* **62**, 1112 (1966).

3. C. de. Visser, W. J. M. Heuvelsland, L. A. Dunn and G. Somsen, *J. Chem. Soc. Faraday Trans.* **74**, 1159 (1978).
4. J. M. G. Cowie and P. M. Toporowski, *Can. J. Chem.* **39**, 2240 (1961).
5. F. Franks (ed.), *Physico - Chemical Processes in Mixed Aqueous Solvents* (Heinemann, London, 1969).
6. J. S. Rowlinson and F. L. Swinton, *Liquids and Liquid Mixtures* (Butterworths, London, 1982).
7. A. S. Kertes (Chief Editor), *Solubility Data Series* (Pergamon Press, New York, 1984).
8. S. Glasstone, *Text Book of Physical Chemistry*, 2nd. edn. (Macmillan, New York, 1991).
9. G. Perron, L. Couture and J. E. Desnoyers, *J. Solution Chem.* **21**, 433 (1992).
10. S. S. N. Murthy, *Cryobiology* **36**, 84 (1998).
11. S. S. N. Murthy and Deepak Kumar, *J. Chem. Soc. Faraday Trans.* **89**, 2423 (1993).
12. S. S. N. Murthy, *J. Phys. Chem. A* **103**, 7927 (1999).
13. S. S. N. Murthy and Madhusudan Tyagi, *J. Solution Chem.* **31**, 33 (2002).
14. S. S. N. Murthy, *J. Phys. Chem. B* **104**, 6955 (2000).
15. S. S. N. Murthy, *J. Phys. Chem. B* **101**, 6043 (1997).
16. N. E. Hill, W. E. Vaughan, A. H. Price and M. Davies, *Dielectric Properties and Molecular Behaviour* (Van Nostrand Peinhold, London, 1969).
17. D. J. Denney and R. H. Cole, *J. Chem. Phys.* **23**, 1767 (1955).

18. D.J. Denney and J.W. Ring, *J. Chem. Phys.* **19**, 1268 (1963).
19. P. Daumezon and R. Heitz, *J. Chem. Phys.* **55**, 5704 (1971).
20. P. Sixou, P. Dansas and D. Gillot, *J. Chem. Phys.* **64**, 834 (1967).
21. P. Sixou, P. Daumezon and P. Dansas, *J. Chem. Phys.* **64**, 824 (1967).
22. B. Gestblom, A. El Samahy and J. Sjoblom, *J. Solution Chem.* **14**, 375 (1985).
23. M. K. Kroeger, *J. Mol. Liquids* **36**, 101 (1987).
24. F. F. Hanna, I. K. Hakima, A. L. C. Saad, F. Hufnagel, and F. Drexler, *J. Mol. Liquids* **49**, 49 (1991).
25. G. P. Johari and C. P. Smyth, *J. Chem. Phys.* **56**, 4411 (1972).
26. G. P. Johari and M. Goldstein, *J. Chem. Phys.* **53**, 2372 (1970).
27. G. P. Johari and M. Goldstein, *J. Chem. Phys.* **55**, 4245 (1971).
28. S. S. N. Murthy, J. Sobhanadri and Gangasharan, *J. Chem. Phys.* **100**, 460 (1994).
29. S. S. N. Murthy, *Phase Transitions* **50**, 63 (1994).
30. S. S. N. Murthy, N. Arya and A. Paikaray, *J. Chem. Phys.* **102**, 8213 (1995).
31. M. F. Shears and G. Williams, *J. Chem. Soc. Faraday Trans.2* **69**, 608 (1973).
32. G. J. Reid and M. W. Evans, *J. Chem. Phys.* **76**, 2576 (1982).
33. (a) D. R. Lide, *CRC Handbook of Physics and Chemistry*, 71st. edn. (CRC Press, Boca Raton, 1990);  
(b) Kirk-othmer, *Encyclopaedia of Chemical Technology*, Vol. 12 (Wiley, New York, 1967).

34. G. S. Parks, S. B. Thomas and D. W. Light, *J. Chem. Phys.* **4**, 64 (1936).
35. V. P. Privalko, *J. Phys. Chem.* **84**, 3306 (1980).
36. C. A. Angell and W. Sichina, *Ann. N. Y. Acad. Sci.* **276**, 53 (1976).
37. C. A. Angell, *J. Non-Cryst. Solids* **131 – 133**, 13 (1991).
38. S. S. N. Murthy, *J. Phys. Chem.* **93**, 3347 (1989).
39. S. S. N. Murthy, *J. Chem. Soc. Faraday Trans. II* **85**, 581 (1989).
40. Madhusudan Tyagi and S. S. N. Murthy, *J. Chem. Phys.* **114**, 3640 (2001).
41. S. Havriliak and S. Negami, *J. Poly. Sci. C* **14**, 99 (1966).
42. R. Lovell, *J. Phys. C. Sol. State Phys.* **7**, 4378 (1974).
43. A. K. Jonscher, *Dielectric Relaxation in Solids* (Chelsea Dielectric Press, Chelsea, London, 1983).
44. F. A. Grant, *J. Appl. Phys.* **29**, 76 (1958).
45. W. Drinkard and D. Kivelson, *J. Amer. Chem. Soc.* **62**, 1494 (1958).
46. U. Kaatze, R. Pottel and M. Sichafer, *J. Phys. Chem.* **93**, 5623 (1989).
47. V. Wessels, M. Stockhausen and G. Schutz, *Z. Phys. Chem. Neue Folge* **168**, 193 (1990).
48. F. Buckley and A. A. Maryott, *Tables of Dielectric Dispersion Data for Pure Liquids and Dilute Solutions* NBS Circular no. 589, 1958.
49. S. M. Puranik, A. C. Kumbarkhane and S. Mehrotra, *J. Chem. Soc. Faraday Trans.* **88**, 433 (1992).
50. C. A. Angell, J. M. Sare and E. J. Sare, *J. Phys. Chem.* **82**, 2622 (1978).



51. S. S. N. Murthy, *Therm. Chem. Acta* **359**, 143 (2000).
52. S. S. N. Murthy, *J. Phys. Chem. B* **100**, 8508, 1996.
53. Gangasharan and S. S. N. Murthy, *J. Chem. Phys.* **99**, 9865 (1993).